Research Paper

Fibroblasts from different body parts exhibit distinct phenotypes in adult progeria Werner syndrome

Hisaya Kato[1,2], Yoshiro Maezawa[1,2], Naoya Takayama[3], Yasuo Ouchi[3,4], Hiyori Kaneko[1,2], Daisuke Kinoshita[1,5], Aki Takada-Watanabe[1], Motohiko Oshima[6], Masaya Koshizaka[1,2], Hideyuki Ogata[7], Yoshitaka Kubota[7], Nobuyuki Mitsukawa[7], Koji Eto[3,8], Atsushi Iwama[6], Koutaro Yokote[1,2]

[1]Department of Endocrinology, Hematology and Gerontology, Chiba University Graduate School of Medicine, Chuo-Ku, Chiba 260-8670, Japan
[2]Division of Diabetes, Metabolism and Endocrinology, Chiba University Hospital, Chuo-Ku, Chiba 260-8670, Japan
[3]Department of Regenerative Medicine, Chiba University Graduate School of Medicine, Chuo-Ku, Chiba 260-8670, Japan
[4]Gene Expression Laboratory, Salk Institute for Biological Studies, La Jolla, CA 92037, USA
[5]Department of Diabetes and Metabolism, Asahi General Hospital, Asahi-Shi, Chiba 289-2511, Japan
[6]Division of Stem Cell and Molecular Medicine, Center for Stem Cell Biology and Regenerative Medicine, The Institute of Medical Science, The University of Tokyo, Minato-Ku, Tokyo 108-8639, Japan
[7]Department of Plastic, Reconstructive, and Aesthetic Surgery, Chiba University Graduate School of Medicine, Chuo-Ku, Chiba 260-8670, Japan
[8]Department of Clinical Application, Center for IPS Cell Research and Application (CiRA), Kyoto University, Shogoin, Sakyo-Ku, Kyoto 606-8507, Japan

Correspondence to: Hisaya Kato, Yoshiro Maezawa, Koutaro Yokote; **email:** hisayakato@chiba-u.jp, yoshiromaezawa@chiba-u.jp, kyokote@faculty.chiba-u.jp
Keywords: Werner syndrome, dermal fibroblasts, adipogenesis, chondrogenesis, osteogenesis
Received: September 5, 2020 **Accepted:** February 8, 2021 **Published:** February 24, 2021

ABSTRACT

Werner syndrome (WS), also known as adult progeria, is characterized by accelerated aging symptoms from a young age. Patients with WS experience painful intractable skin ulcers with calcifications in their extremities, subcutaneous lipoatrophy, and sarcopenia. However, there is no significant abnormality in the trunk skin, where the subcutaneous fat relatively accumulates. The cause of such differences between the limbs and trunk is unknown. To investigate the underlying mechanism behind these phenomena, we established and analyzed dermal fibroblasts from the foot and trunk of two WS patients. As a result, WS foot-derived fibroblasts showed decreased proliferative potential compared to that from the trunk, which correlated with the telomere shortening. Transcriptome analysis showed increased expression of genes involved in osteogenesis in the foot fibroblasts, while adipogenic and chondrogenic genes were downregulated in comparison with the trunk. Consistent with these findings, the adipogenic and chondrogenic differentiation capacity was significantly decreased in the foot fibroblasts *in vitro*. On the other hand, the osteogenic potential was mutually maintained and comparable in the foot and trunk fibroblasts. These distinct phenotypes in the foot and trunk fibroblasts are consistent with the clinical symptoms of WS and may partially explain the underlying mechanism of this disease phenotype.

INTRODUCTION

Werner syndrome (WS) is a rare autosomal recessive premature aging disorder that begins at a young age with graying and loss of hair and cataracts, followed by accelerated aging symptoms such as diabetes, atherosclerosis, and cancer [1–4]. The median life expectancy is in the mid-50s, and most deaths are due to arteriosclerosis and malignancy [5]. Owing to the founder mutation, a high incidence of WS is observed in Japan [6, 7].

The causative gene is WRN, which is located on chromosome 8 and is involved in DNA replication, DNA repair, and telomere maintenance [8]. WS fibroblasts with deficient or dysfunctional WRN proteins show premature cellular senescence *in vitro* [9]. This phenotype is largely dependent on telomere shortening and can be overcome by telomerase overexpression [10, 11].

WS mimics various symptoms of general aging. However, there are also phenotypes specific to WS, such as refractory skin ulcers with severe pain in the extremities, which affect over 80% of patients and may even result in limb amputation [12]. Common sites for ulceration are the heels, soles, toes, Achilles tendons, and elbows. Painful subcutaneous calcification has been reported to precede skin ulcers [13]. The atrophy of subcutaneous fat and muscle when present in the extremities resembles branches of dried trees, which is diagnosed as sarcopenia [14]. In contrast, there is an accumulation of subcutaneous fat in the trunk [15, 16]. While the skin of the extremities, frequently accompanied by ulcers, is atrophic and tight, that of the trunk retains its elasticity and does not develop ulcers. The underlying mechanism behind these differences remains unknown.

To clarify the relationship between the skin properties and the high prevalence of skin ulcers in the extremities, we established fibroblasts from the skin of the trunk and that of the foot from the vicinity of ulceration in two WS patients.

RESULTS

Foot fibroblasts exhibited reduced proliferation compared to the trunk fibroblasts in a telomere-dependent manner

In WS, the skin in the extremities atrophies and hardens, and a skin ulcer develops, while there is no obvious abnormality in the trunk skin. Therefore, plastic surgery is often performed to graft skin from the trunk to the ulcer site in order to treat the skin ulcers. In this study, we established fibroblasts from the foot skin (normal skin adjacent to the ulcer) and trunk skin (graft) of two WS patients (WS1 and WS2) who were admitted to our hospital for plastic surgery. We hypothesized that the difference in skin symptoms between the limb and trunk was related to a reduced proliferative capacity of the limb fibroblasts compared to that of the trunk. As expected, the proliferation rate of foot skin-derived fibroblasts was lower than that of the trunk (Figure 1A). In previous reports, the cause of the reduced proliferative potential of WS fibroblasts was explained by shortened telomere length [10, 11]. Consistent with these reports, there was a significant difference in the telomere lengths between the foot and trunk fibroblasts (Figure 1B, 1C and Supplementary Figure 1). These results suggest that the difference in proliferation ability between skin fibroblasts of the foot and trunk is dependent on the telomere length.

Foot and trunk fibroblasts in WS showed differential expression of genes, especially those involved in embryogenesis and differentiation

Next, transcriptome analysis was performed using RNA sequences to characterize the gene expression profiles of the foot and trunk fibroblasts. In the hierarchical clustering analysis, the WS foot and trunk fibroblasts were classified into different clusters beyond individual differences (Supplementary Figure 2A and Supplementary Table 1). The analysis of differentially expressed genes (DEGs) was performed to identify genes with more than 2-fold differences in expression, and a total of 140 up-regulated and 119 down-regulated genes were identified in the foot (Figure 2A and Supplementary Tables 2, 3). Enrichment analysis of DEGs revealed that their pathways are mainly involved in differentiation and embryogenesis (Figure 2B). Among them, Homeobox A13 (HOXA13) was explicitly expressed in the foot, while Homeobox B5 (HOXB5), Homeobox B6 (HOXB6), Homeobox B7 (HOXB7), and Homeobox D4 (HOXD4) expression were specific to the trunk (Figure 2C), which is consistent with the site-specific gene expression of fibroblasts from normal individuals in previous reports [17, 18]. Intriguingly, the foot fibroblasts showed an elevated expression of genes that relate to the promotion of osteogenesis and suppression of adipogenesis and chondrogenesis, including Stathmin 2 (STMN2), Copine 7 (CPNE7), Protein Tyrosine Phosphatase Receptor Type B (PTPRB), Solute Carrier Family 2 Member 5 (SLC2A5), and HOXA Distal Transcript Antisense RNA (HOTTIP) (Figure 2C) [19–23]. In contrast, in the fibroblasts of the trunk, the expression of the following genes were increased; Clusterin (CLU), Peroxisome Proliferator-Activated Receptor Gamma (PPARG), Insulin-Like Growth Factor 2 MRNA

Binding Protein 3 (IGF2BP3), Cysteine Dioxygenase Type 1 (CDO1), and Zinc Finger Protein, FOG Family Member 2 (ZFPM2) (Figure 2C), which are associated with the promotion of adipogenesis or chondrogenesis and suppression of osteogenesis [24–29]. However, regarding senescence-associated genes, no significant differences were observed in the expression of Cyclin-Dependent Kinase Inhibitor 1A (CDKN1A, p21) and Cyclin-Dependent Kinase Inhibitor 2A (CDKN2A, p16) (Supplementary Figure 2B) [30, 31]. These results suggest that the foot and trunk fibroblasts in WS have distinct gene expressions that regulate mesenchymal-lineage differentiation, but these differences are independent of cellular senescence.

Foot fibroblasts in WS were less capable of adipogenesis compared with the trunk

WS patients present with subcutaneous lipoatrophy in the extremities, while subcutaneous fat tends to accumulate in the trunk. Several reports have previously shown that human dermal fibroblasts can differentiate into mesodermal lineages *in vitro*, including adipocytes [32–34]. Taken together with the above results, we hypothesized that the adipogenesis potential is lower in foot fibroblasts than in the trunk. Thus, we investigated the adipogenic capacity of WS fibroblasts by culturing them in the adipogenic differentiation medium. After induction of adipogenesis, Oil red O staining results

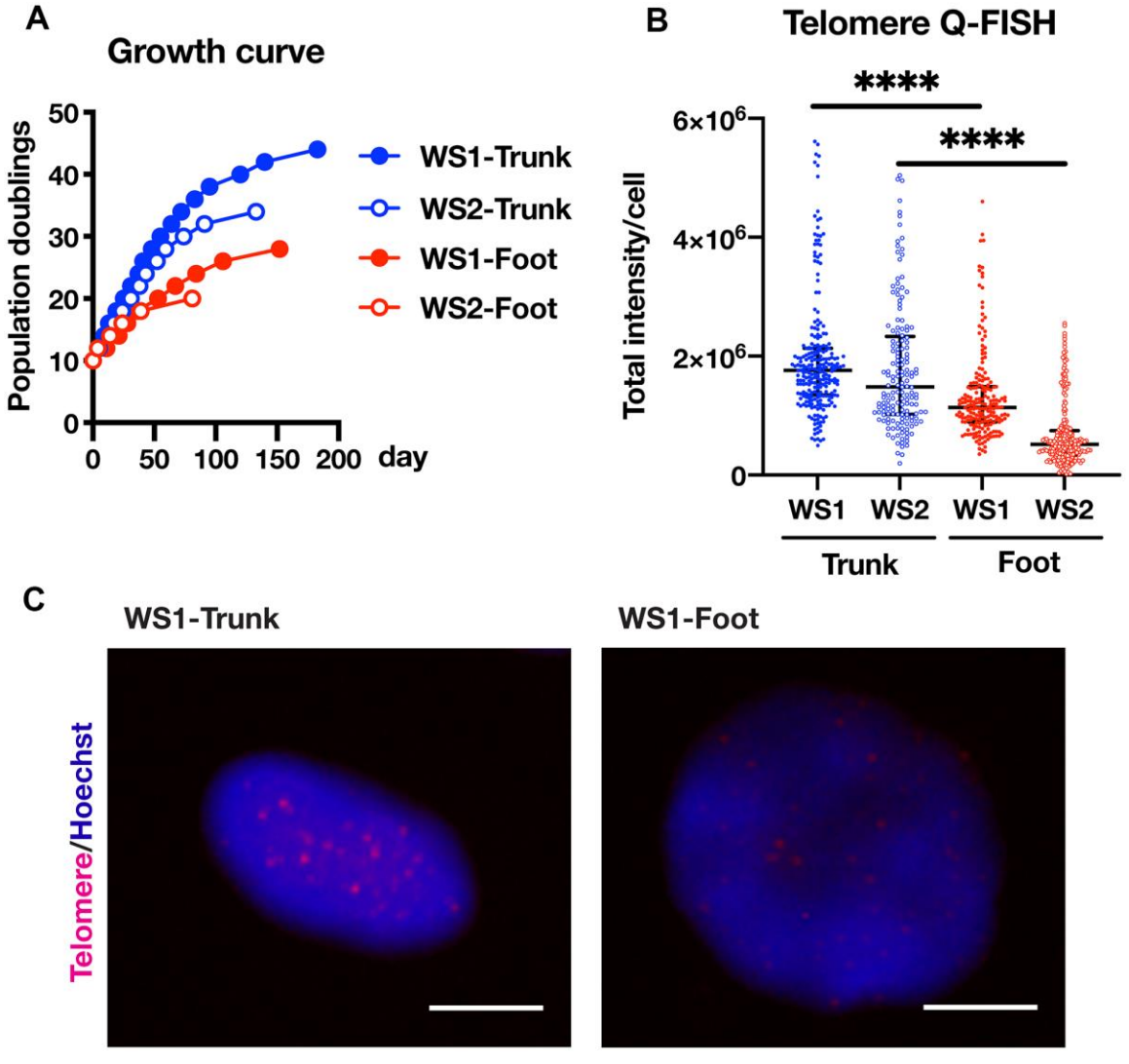

Figure 1. Foot fibroblasts exhibited reduced proliferative capacity compared to that from the trunk in a telomere length-dependent manner. (**A**) Growth curves of the fibroblasts from the trunk and foot in two WS patients. (**B**) Telomere length quantification through Q-FISH. Data are median values ± interquartile range of each cell line. More than 150 cells for each cell line were analyzed. For statistical analysis, Mann Whitney test was performed (****p<0.0001). (**C**) Representative image of telomere Q-FISH of WS1. Bar = 10 μm.

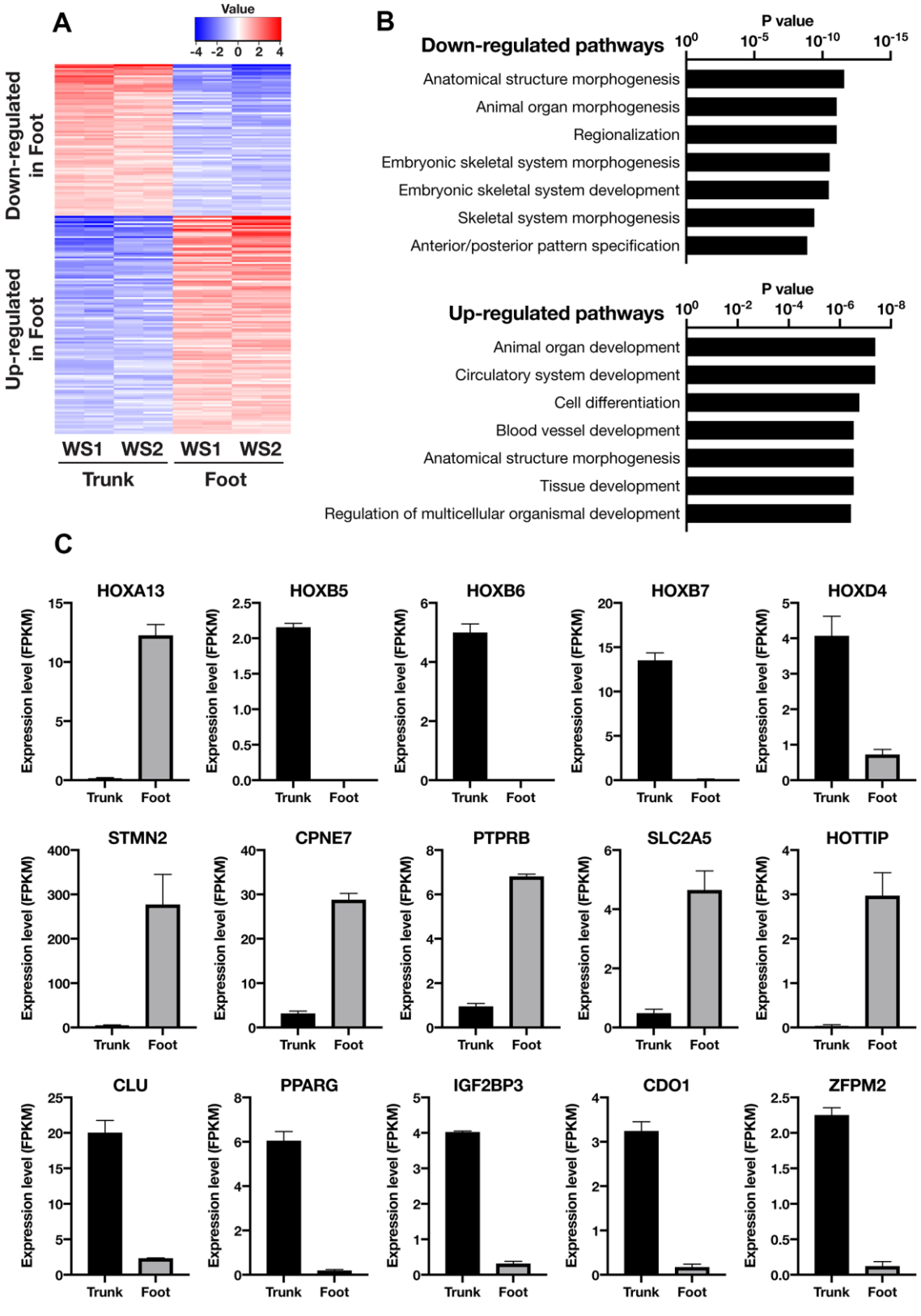

Figure 2. Transcriptome analysis showed distinct gene expression profiles between the trunk and foot fibroblasts. (**A**) Heatmap of differentially expressed genes between the trunk and foot. Cutoff: |log2(Foot/Trunk)| > 1 and FDR < 0.05. (**B**) List of the top seven Gene Ontology (GO: biological process) terms and corresponding p values related to Figure 2A. (**C**) Differentially expressed genes specifically involved in embryonic development and mesenchymal cell differentiation. Data are means ± SEM of two patients (technically n=2 in each sample).

showed foot fibroblasts with significantly fewer oil droplets than the trunk (Figure 3A, 3B and Supplementary Figure 3). In gene expression analysis by qRT-PCR, adipocyte marker genes, PPARG, Fatty Acid Binding Protein 4 (FABP4), CCAAT Enhancer Binding Protein Alpha (CEBPA), and Leptin (LEP) were significantly decreased in the foot group compared with the trunk (Figure 3C) [35]. These results indicate that the trunk fibroblasts of WS maintain adipogenic capacity but the foot fibroblasts do not.

Foot fibroblasts in WS exhibited an attenuated capacity for chondrogenesis

Next, we performed chondrogenic differentiation to confirm a disparity in chondrogenesis between the trunk and foot fibroblasts. After the induction of chondrogenesis using the pellet method, the spheroid diameter was significantly smaller in the foot fibroblasts from WS1 than in the trunk group (Figure 4A, 4B). On the other hand, WS2 foot fibroblasts failed to maintain spheroid morphology (Supplementary Figure 4). The chondrogenesis differentiation marker, SRY-Box Transcription Factor 9 (SOX9), was significantly decreased in the foot group, and this tendency was also observed for Aggrecan (ACAN) (Figure 4C) [36]. These results suggest that WS foot fibroblasts tend to have a reduced capacity for chondrogenic differentiation compared with the trunk.

Foot and trunk fibroblasts in WS were equally capable of osteogenesis

Next, the osteogenic differentiation ability was compared. After culturing in the osteogenesis medium, no clear difference was observed in the Alizarin red-

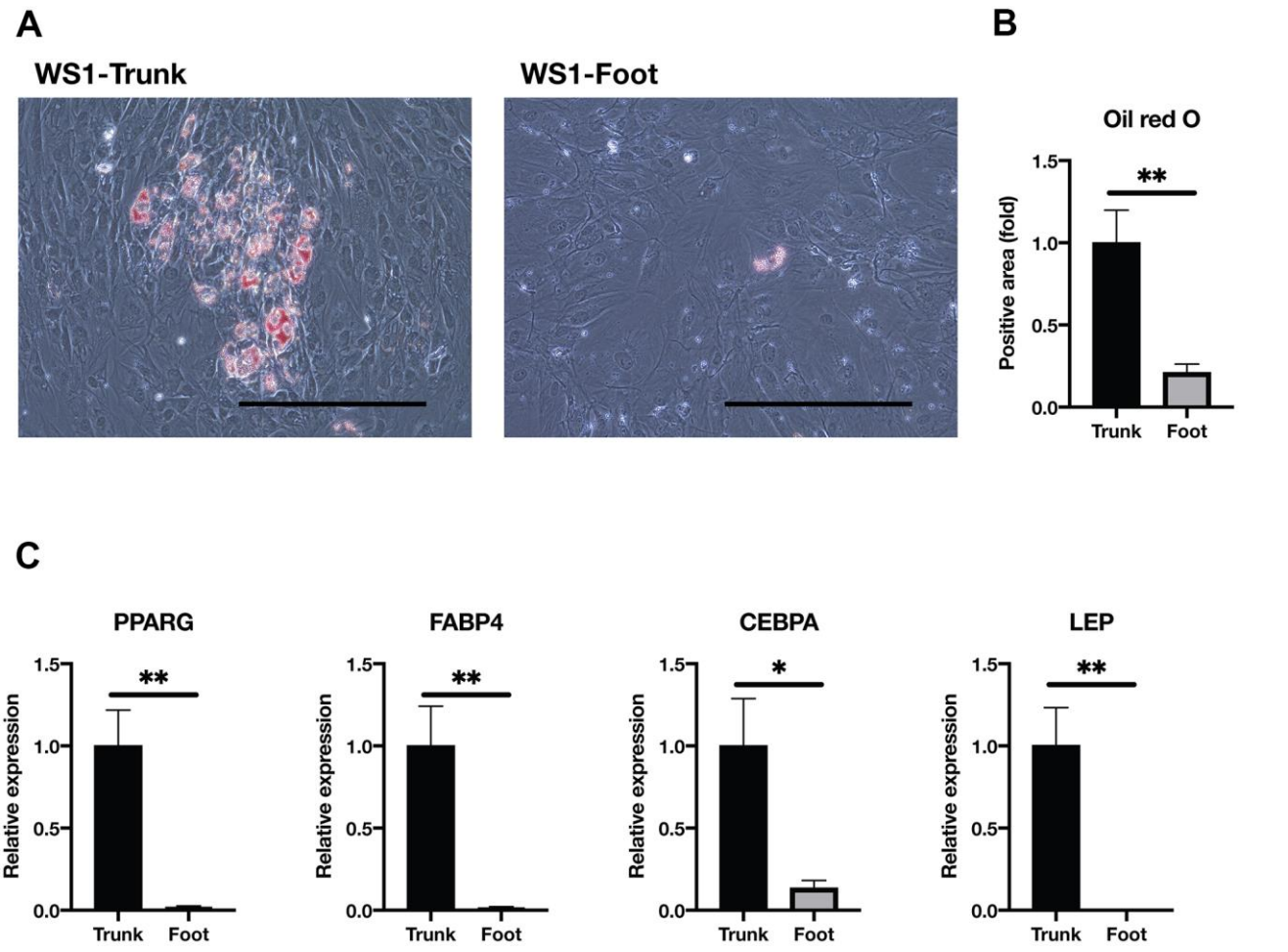

Figure 3. Adipogenesis was impaired in the foot fibroblasts. (**A**) Representative images of Oil red O staining after two weeks induction of adipogenesis in the trunk and foot fibroblasts of WS1. Bar = 300 μm. (**B**) Quantification of relative Oil red O staining area. Data are means ± SEM of two patients from four microscopic views. For statistical analysis, student t-test was performed (**p<0.01). (**C**) Relative gene expression analyzed by qRT-PCR. Data are means ± SEM of two patients with three technical replicates. For statistical analysis, student t-test was performed (*p<0.05; **p<0.01).

stained area between the trunk and foot groups (Figure 5A, 5B and Supplementary Figure 5). The expression of Alkaline Phosphatase, Biomineralization Associated (ALPL), a marker of osteogenesis, was significantly elevated in the foot group (Figure 5C). On the other hand, RUNX Family Transcription Factor 2 (RUNX2) expression was significantly elevated in the trunk group, and there were no significant differences in other differentiation markers (Secreted Phosphoprotein 1, SPP1; Collagen Type I Alpha 1 Chain, COL1A1) (Figure 5C) [37]. These results suggest that foot fibroblasts in WS maintain the equivalent level of osteogenic differentiation capacity to the trunk.

DISCUSSION

This is the first report comparing the phenotypes of dermal fibroblasts taken from different parts of the body of the same WS patient. The WS foot fibroblasts showed a reduced proliferative capacity with shorter telomeres, in comparison to the trunk fibroblasts. Transcriptome analysis showed increased gene

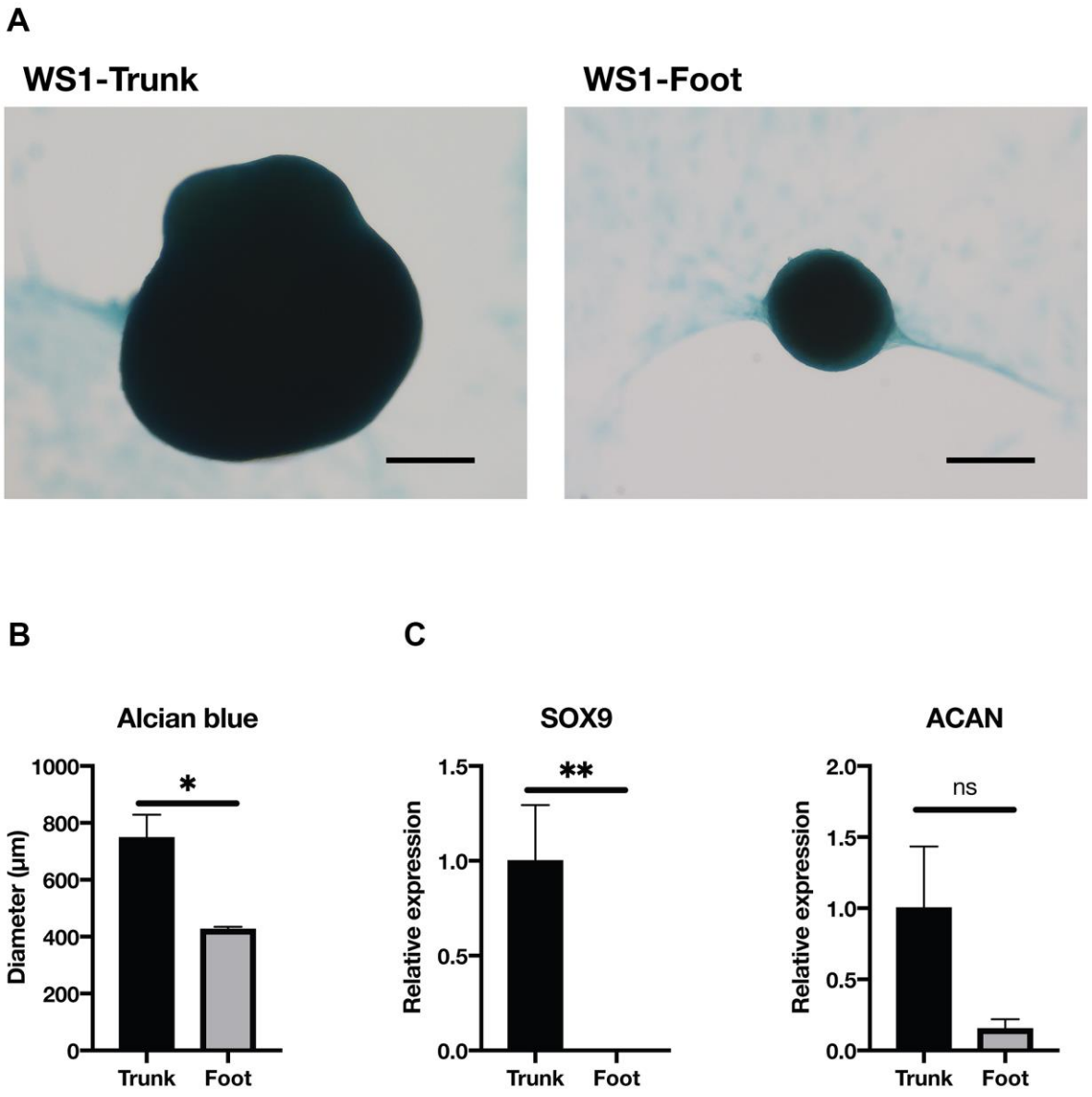

Figure 4. Chondrogenesis tended to be reduced in the foot fibroblasts. (**A**) Representative images of Alcian blue staining after two weeks induction of chondrogenesis in the trunk and foot fibroblasts of WS1. Bar = 300 μm. (**B**) Quantification of the diameter of chondrogenic spheroids. WS1-trunk, WS2-trunk, and WS1-foot were included. Data are means ± SEM. For statistical analysis, student t-test was performed (*p<0.05). (**C**) Relative gene expression analyzed by qRT-PCR. Data are means ± SEM of two patients with three technical replicates. For statistical analysis, student t-test was performed (ns, not significant; *p<0.05; **p<0.01).

expression related to osteogenic differentiation in the foot group and that of adipogenic and chondrogenic differentiation in the trunk group. Indeed, *in vitro* induction of adipogenesis and chondrogenesis of the foot fibroblasts showed significantly reduced differentiation capacity compared with the trunk. However, there was no difference in osteogenic capacity between the trunk and foot fibroblasts.

Previously, Rinn et al. conducted transcriptome analyses among normal human fibroblasts taken from different sites in the body [17, 18]. Among the DEGs between the extremities and trunk, the expression distribution of HOX genes is consistent with cell migration during human development [38]. Rinn et al. identified that HOXA13 was explicitly up-regulated in foot-derived fibroblasts, while the HOXB gene cluster was trunk-specific [17, 18]; these data are consistent with our results.

However, most of the genes we extracted through the DEG analysis in this study did not show site-specific changes in the previous reports [17, 18]. PPARG, which we found to be up-regulated in the trunk fibroblasts of the WS patients, is a master regulator of adipogenesis, and its overexpression promotes adipose differentiation [39]. In this study, the WS trunk-derived fibroblasts showed higher PPARG expression than the foot-derived ones, and there was a clear difference in the *in vitro* adipose differentiation ability. These apparent

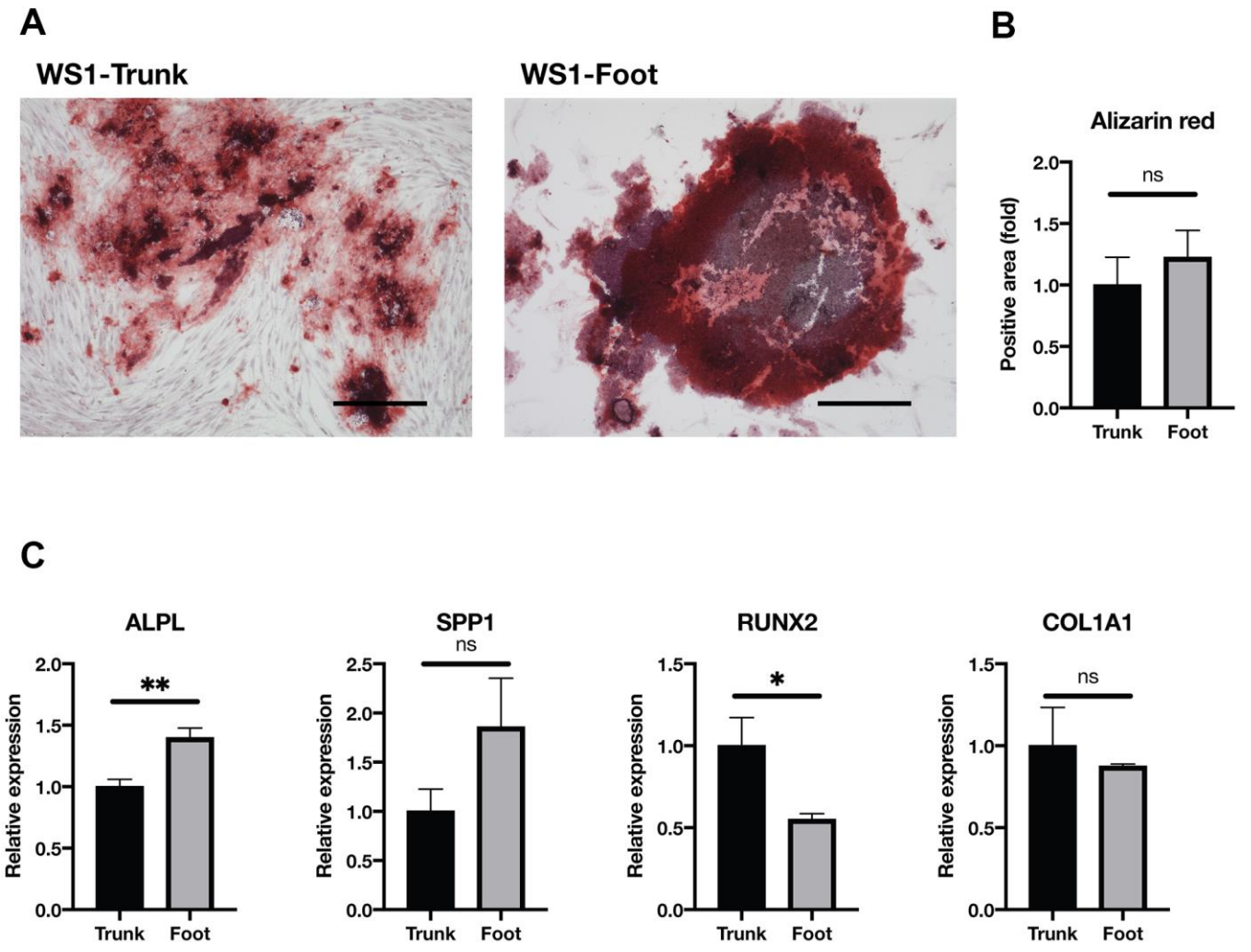

Figure 5. Osteogenesis was maintained in both groups. (**A**) Representative images of Alizarin red staining two weeks after induction of osteogenesis in the trunk and foot fibroblasts of WS1. Bar = 300 μm. (**B**) Quantification of relative stained area with Alizarin red. Data are means ± SEM of two patients with four microscopic views. For statistical analysis, student t-test was performed (ns, not significant). (**C**) Relative gene expression analyzed by qRT-PCR. Data are means ± SEM of two patients with three technical replicates. For statistical analysis, student t-test was performed (ns, not significant; *p<0.05; **p<0.01).

discrepancies are reminiscent of WS phenotypes, namely the trunk with relatively abundant subcutaneous fat and the extremities with lipoatrophy [15, 16]. In addition, although the anatomic origin of the fibroblast is unclear, WRN-depleted fibroblasts exhibit upregulation of PPARG [40]. Taken together with our findings, these results suggest that the regulation of PPARG gene expression in WRN-depleted cells might be context-dependent and that they can be down-regulated in the fibroblasts in the disease site. Further research is needed to understand the mechanism of downregulation of PPARG in WS foot fibroblasts compared to the WS trunk-derived fibroblasts. In addition, STMN2, a marker of osteogenesis, which is up-regulated during the osteogenic induction of mesenchymal stem cells [19], is the gene with the most distinct regulation in this study: the expression was overwhelmingly increased in the foot fibroblasts compared with the trunk.

Honjo et al. reported that painful subcutaneous calcification precedes skin ulcers in WS patients [13]. Patients with WS frequently suffer painful clavus and callus on the feet, which leads to the development of intractable skin ulcers [1, 12]. Ectopic soft tissue calcification also occurs in the limbs of WS patients [41]. Considering our findings that WS foot fibroblasts have a diminished ability to differentiate into adipocytes and chondrocytes while their osteogenic differentiation capacity remains fully preserved, the ossification of fibroblasts in the dermal and subcutaneous layers of the skin may result in these symptoms. In addition, reversible direct conversion of subcutaneous adipocytes into fibroblasts, *in vivo*, has been reported [42–44]. Therefore, our results suggest the possibility that subcutaneous lipoatrophy in WS extremities might attribute to the inability of adipogenic differentiation in fibroblasts in the disease site.

In this study, we revealed the distinct gene expression profiles and phenotypes in WS dermal fibroblasts derived from the foot and trunk. This study highlights the relationship between fibroblast phenotypes and WS-specific symptoms, refractory skin ulcers and subcutaneous lipoatrophy in extremities. These results could lead to a further understanding of the disease's mechanism and development of a new therapeutic strategy in the future.

MATERIALS AND METHODS

Establishment of fibroblasts and cell culture

WS dermal fibroblasts were established from two WS patients (WS1 and WS2, Supplementary Table 4). Both were hospitalized for treatment of their foot skin ulcers, and the skin graft was taken from the trunk (groin). The healthy skin neighboring the ulcer and the skin partly taken from the graft were explanted into a dish as previously described [45]. Cell culture was performed with DMEM (043-30085, Wako, Osaka, Japan), supplemented with 10% FBS (10270106, Gibco, Waltham, MA, U.S.A), and antibiotic-antimycotic (15240062, Gibco) in humidified 5% CO_2 air. The medium was changed every two days. When reaching sub-confluency, cells were passaged at a 1:4 split ratio until growth arrest and population doublings were calculated.

Telomere quantitative fluorescence *in situ* hybridization (Q-FISH)

Fibroblasts at PD10 were treated with the colcemid kit (Chromocenter, Tottori, Japan) and fixed in Carnoy's solution following the manufacturer's protocol. The fixed cells on coverslips were treated with ribonuclease (312-01931, Nippon Gene, Tokyo, Japan) and 0.005 % pepsin (V1959, Promega, WI, U.S.), hybridized with peptide nucleic acid oligonucleotide probes (F1002, Panagene, Daejeon, South Korea), and immuno-stained with Hoechst 33342 (H342, Dojindo, Kumamoto, Japan), according to the manufacturer's protocols. Images were recorded using a BZ-X700 microscope (Keyence, Osaka, Japan). Quantification was performed using the Telometer (https://demarzolab.pathology.jhmi.edu/telometer/), as previously described [46, 47].

Quantitative polymerase chain reaction (qPCR)

RNA was extracted and reverse-transcribed, as previously described [48]. TaqMan Gene Expression Assays for PPARG (Hs01115513_m1), FABP4 (Hs01086177_m1), CEBPA (Hs00269972_s1), LEP (Hs00174877_m1), SOX9 (Hs00165814_m1), ACAN (Hs00153936_m1), ALPL (Hs01029144_m1), SPP1 (Hs00959010_m1), RUNX2 (Hs01047973_m1), COL1A1 (Hs00164004_m1), and B2M (Hs00187842_m1) were purchased from Applied Biosystems (Waltham, MA, U.S.). Quantification was performed with the ⊿⊿Ct method using B2M as an internal control.

Tri-lineage differentiation

In vitro differentiation potentials of the fibroblasts into three mesenchymal lineages were evaluated by using adipogenesis, chondrogenesis, and osteogenesis differentiation kits (A1007001, A1007101, and A1007201, respectively; Gibco) according to manufacturer's protocols. Cells at PD 9 to 10 were used. After two weeks of differentiation, cells were sampled and stained. For each staining assay, Oil red O, Alcian

blue, and Alizarin red staining (Sigma-Aldrich, St. Louis, MO, U.S.A) were used, respectively. Quantification of the stains was performed using a BZ-X700 microscope (Keyence, Osaka, Japan).

Transcriptome analysis

mRNA was extracted from fibroblasts at PD 10 and the cDNA library was synthesized using the NEBNext Ultra RNA Library Prep Kit (E7370S, New England BioLabs, Beverly, MA, U.S.A). Sequencing was carried out (technically n=2 in each sample) by HiSeq1500 (Illumina, San Diego, CA, U.S.A) with 60bp single-reads. The reference genome mapping (UCSC/hg19) was performed using TopHat (version 2.0.13; with default parameters) with annotation data from iGenomes (Illumina). Cuffdiff (Cufflinks version 2.2.1; with default parameters) was used to quantify the gene expression levels. FPKM data were analyzed by iDEP (http://bioinformatics.sdstate.edu/idep/) as described by the authors [49].

Study approval

All experiments were approved by the institutional review boards at the Chiba University Graduate School of Medicine (Chiba, Japan). Written informed consent was obtained from study participants before the commencement of this research.

Abbreviations

DEG: differentially expressed gene; FDR: false discovery rate; FPKM: fragments per kilobase million; PD: population doublings; Q-FISH: quantitative fluorescence *in situ* hybridization; qRT-PCR: quantitative reverse transcription polymerase chain reaction; SEM: standard error of the mean; WS: Werner syndrome.

AUTHOR CONTRIBUTIONS

H.Kato, Y.M., and K.Y. designed the study, analyzed the data, and wrote the manuscript; H.Kato carried out the experiments and made the figures; N.T., M.O., and A.I. conducted transcriptome analysis; Y.O., M.K., and K.E. discussed the data; H.Kaneko, D.K., and A.T.W. carried out the experiments; H.O., Y.K., and N.M. conducted sampling from patients; all authors approved the final version of the manuscript.

ACKNOWLEDGMENTS

We want to thank Ms. Naoko Tomoda (Department of Endocrinology, Hematology and Gerontology, Chiba University Graduate School of Medicine, Chiba, Japan) for supporting the funding management.

CONFLICTS OF INTEREST

The authors declare that they have no conflicts of interest.

FUNDING

This work was supported by Japan Society for the Promotion of Science (JSPS) KAKENHI under Grant Numbers JP19K23939 (H.Kato), JP20H00524 (K.Y.), JP20K16542 (H.Kato); Japan Agency for Medical Research and Development (AMED) under Grant Numbers JP20bm0804016 (K.Y.), JP20ek0109353 (K.Y.), JP20gm5010002 (K.Y.); Ministry of Health, Labour and Welfare (MHLW) of Japan under Grant Number H30-nanchi-ippan-009 (K.Y.).

REFERENCES

1. Oshima J, Sidorova JM, Monnat RJ Jr. Werner syndrome: clinical features, pathogenesis and potential therapeutic interventions. Ageing Res Rev. 2017; 33:105–14. https://doi.org/10.1016/j.arr.2016.03.002 PMID:26993153

2. Muftuoglu M, Oshima J, von Kobbe C, Cheng WH, Leistritz DF, Bohr VA. The clinical characteristics of Werner syndrome: molecular and biochemical diagnosis. Hum Genet. 2008; 124:369–77. https://doi.org/10.1007/s00439-008-0562-0 PMID:18810497

3. Hisama FM, Oshima J, Martin GM. How research on human progeroid and antigeroid syndromes can contribute to the longevity dividend initiative. Cold Spring Harb Perspect Med. 2016; 6:a025882. https://doi.org/10.1101/cshperspect.a025882 PMID:26931459

4. Monnat RJ Jr. "…Rewritten in the skin": clues to skin biology and aging from inherited disease. J Invest Dermatol. 2015; 135:1484–90. https://doi.org/10.1038/jid.2015.88 PMID:25810110

5. Huang S, Lee L, Hanson NB, Lenaerts C, Hoehn H, Poot M, Rubin CD, Chen DF, Yang CC, Juch H, Dorn T, Spiegel R, Oral EA, et al. The spectrum of WRN mutations in Werner syndrome patients. Hum Mutat. 2006; 27:558–67. https://doi.org/10.1002/humu.20337 PMID:16673358

6. Yokote K, Chanprasert S, Lee L, Eirich K, Takemoto M, Watanabe A, Koizumi N, Lessel D, Mori T, Hisama FM, Ladd PD, Angle B, Baris H, et al. WRN mutation update:

mutation spectrum, patient registries, and translational prospects. Hum Mutat. 2017; 38:7–15. https://doi.org/10.1002/humu.23128 PMID:27667302

7. Satoh M, Imai M, Sugimoto M, Goto M, Furuichi Y. Prevalence of Werner's syndrome heterozygotes in Japan. Lancet. 1999; 353:1766. https://doi.org/10.1016/S0140-6736(98)05869-3 PMID:10347997

8. Rossi ML, Ghosh AK, Bohr VA. Roles of Werner syndrome protein in protection of genome integrity. DNA Repair (Amst). 2010; 9:331–44. https://doi.org/10.1016/j.dnarep.2009.12.011 PMID:20075015

9. Faragher RG, Kill IR, Hunter JA, Pope FM, Tannock C, Shall S. The gene responsible for Werner syndrome may be a cell division "counting" gene. Proc Natl Acad Sci USA. 1993; 90:12030–34. https://doi.org/10.1073/pnas.90.24.12030 PMID:8265666

10. Wyllie FS, Jones CJ, Skinner JW, Haughton MF, Wallis C, Wynford-Thomas D, Faragher RG, Kipling D. Telomerase prevents the accelerated cell ageing of Werner syndrome fibroblasts. Nat Genet. 2000; 24:16–17. https://doi.org/10.1038/71630 PMID:10615119

11. Shimamoto A, Kagawa H, Zensho K, Sera Y, Kazuki Y, Osaki M, Oshimura M, Ishigaki Y, Hamasaki K, Kodama Y, Yuasa S, Fukuda K, Hirashima K, et al. Reprogramming suppresses premature senescence phenotypes of Werner syndrome cells and maintains chromosomal stability over long-term culture. PLoS One. 2014; 9:e112900. https://doi.org/10.1371/journal.pone.0112900 PMID:25390333

12. Takemoto M, Mori S, Kuzuya M, Yoshimoto S, Shimamoto A, Igarashi M, Tanaka Y, Miki T, Yokote K. Diagnostic criteria for Werner syndrome based on Japanese nationwide epidemiological survey. Geriatr Gerontol Int. 2013; 13:475–81. https://doi.org/10.1111/j.1447-0594.2012.00913.x PMID:22817610

13. Honjo S, Yokote K, Fujimoto M, Takemoto M, Kobayashi K, Maezawa Y, Shimoyama T, Satoh S, Koshizaka M, Takada A, Irisuna H, Saito Y. Clinical outcome and mechanism of soft tissue calcification in Werner syndrome. Rejuvenation Res. 2008; 11:809–19. https://doi.org/10.1089/rej.2007.0649 PMID:18729813

14. Yamaga M, Takemoto M, Shoji M, Sakamoto K, Yamamoto M, Ishikawa T, Koshizaka M, Maezawa Y, Kobayashi K, Yokote K. Werner syndrome: a model for sarcopenia due to accelerated aging. Aging (Albany NY). 2017; 9:1738–44. https://doi.org/10.18632/aging.101265 PMID:28738022

15. Mori S, Murano S, Yokote K, Takemoto M, Asaumi S, Take A, Saito Y. Enhanced intra-abdominal visceral fat accumulation in patients with werner's syndrome. Int J Obes Relat Metab Disord. 2001; 25:292–95. https://doi.org/10.1038/sj.ijo.0801529 PMID:11410834

16. Donadille B, D'Anella P, Auclair M, Uhrhammer N, Sorel M, Grigorescu R, Ouzounian S, Cambonie G, Boulot P, Laforêt P, Carbonne B, Christin-Maitre S, Bignon YJ, Vigouroux C. Partial lipodystrophy with severe insulin resistance and adult progeria Werner syndrome. Orphanet J Rare Dis. 2013; 8:106. https://doi.org/10.1186/1750-1172-8-106 PMID:23849162

17. Rinn JL, Bondre C, Gladstone HB, Brown PO, Chang HY. Anatomic demarcation by positional variation in fibroblast gene expression programs. PLoS Genet. 2006; 2:e119. https://doi.org/10.1371/journal.pgen.0020119 PMID:16895450

18. Rinn JL, Wang JK, Liu H, Montgomery K, van de Rijn M, Chang HY. A systems biology approach to anatomic diversity of skin. J Invest Dermatol. 2008; 128:776–82. https://doi.org/10.1038/sj.jid.5700986 PMID:18337710

19. Chiellini C, Grenningloh G, Cochet O, Scheideler M, Trajanoski Z, Ailhaud G, Dani C, Amri EZ. Stathmin-like 2, a developmentally-associated neuronal marker, is expressed and modulated during osteogenesis of human mesenchymal stem cells. Biochem Biophys Res Commun. 2008; 374:64–68. https://doi.org/10.1016/j.bbrc.2008.06.121 PMID:18611392

20. Choung HW, Lee DS, Lee JH, Shon WJ, Lee JH, Ku Y, Park JC. Tertiary dentin formation after indirect pulp capping using protein CPNE7. J Dent Res. 2016; 95:906–12. https://doi.org/10.1177/0022034516639919 PMID:27013639

21. Kim JS, Kim WK, Oh KJ, Lee EW, Han BS, Lee SC, Bae KH. Protein tyrosine phosphatase, receptor type B (PTPRB) inhibits brown adipocyte differentiation through regulation of VEGFR2 phosphorylation. J Microbiol Biotechnol. 2019; 29:645–50. https://doi.org/10.4014/jmb.1810.10033 PMID:30845793

22. Ambrosi TH, Scialdone A, Graja A, Gohlke S, Jank AM, Bocian C, Woelk L, Fan H, Logan DW, Schürmann A,

Saraiva LR, Schulz TJ. Adipocyte accumulation in the bone marrow during obesity and aging impairs stem cell-based hematopoietic and bone regeneration. Cell Stem Cell. 2017; 20:771–84.e6. https://doi.org/10.1016/j.stem.2017.02.009 PMID:28330582

23. Mao G, Kang Y, Lin R, Hu S, Zhang Z, Li H, Liao W, Zhang Z. Long non-coding RNA HOTTIP promotes CCL3 expression and induces cartilage degradation by sponging miR-455-3p. Front Cell Dev Biol. 2019; 7:161. https://doi.org/10.3389/fcell.2019.00161 PMID:31508417

24. Lee EJ, Jan AT, Baig MH, Ahmad K, Malik A, Rabbani G, Kim T, Lee IK, Lee YH, Park SY, Choi I. Fibromodulin and regulation of the intricate balance between myoblast differentiation to myocytes or adipocyte-like cells. FASEB J. 2018; 32:768–81. https://doi.org/10.1096/fj.201700665R PMID:28974563

25. Akune T, Ohba S, Kamekura S, Yamaguchi M, Chung UI, Kubota N, Terauchi Y, Harada Y, Azuma Y, Nakamura K, Kadowaki T, Kawaguchi H. PPARgamma insufficiency enhances osteogenesis through osteoblast formation from bone marrow progenitors. J Clin Invest. 2004; 113:846–55. https://doi.org/10.1172/JCI19900 PMID:15067317

26. Wang Y, Liu Y, Fan Z, Liu D, Wang F, Zhou Y. IGFBP2 enhances adipogenic differentiation potentials of mesenchymal stem cells from wharton's jelly of the umbilical cord via JNK and Akt signaling pathways. PLoS One. 2017; 12:e0184182. https://doi.org/10.1371/journal.pone.0184182 PMID:28859160

27. Deng P, Chen Y, Ji N, Lin Y, Yuan Q, Ye L, Chen Q. Cysteine dioxygenase type 1 promotes adipogenesis via interaction with peroxisome proliferator-activated receptor gamma. Biochem Biophys Res Commun. 2015; 458:123–27. https://doi.org/10.1016/j.bbrc.2015.01.080 PMID:25637537

28. Zhao X, Deng P, Feng J, Wang Z, Xiang Z, Han X, Bai D, Pae EK. Cysteine dioxygenase type 1 inhibits osteogenesis by regulating Wnt signaling in primary mouse bone marrow stromal cells. Sci Rep. 2016; 6:19296. https://doi.org/10.1038/srep19296 PMID:26763277

29. Huang J, Peng J, Cao G, Lu S, Liu L, Li Z, Zhou M, Feng M, Shen H. Hypoxia-induced MicroRNA-429 promotes differentiation of MC3T3-E1 osteoblastic cells by mediating ZFPM2 expression. Cell Physiol Biochem. 2016; 39:1177–86. https://doi.org/10.1159/000447824 PMID:27576955

30. López-Otín C, Blasco MA, Partridge L, Serrano M, Kroemer G. The hallmarks of aging. Cell. 2013; 153:1194–217. https://doi.org/10.1016/j.cell.2013.05.039 PMID:23746838

31. Hernandez-Segura A, Nehme J, Demaria M. Hallmarks of cellular senescence. Trends Cell Biol. 2018; 28: 436–53. https://doi.org/10.1016/j.tcb.2018.02.001 PMID:29477613

32. Blasi A, Martino C, Balducci L, Saldarelli M, Soleti A, Navone SE, Canzi L, Cristini S, Invernici G, Parati EA, Alessandri G. Dermal fibroblasts display similar phenotypic and differentiation capacity to fat-derived mesenchymal stem cells, but differ in anti-inflammatory and angiogenic potential. Vasc Cell. 2011; 3:5. https://doi.org/10.1186/2045-824X-3-5 PMID:21349162

33. Junker JP, Sommar P, Skog M, Johnson H, Kratz G. Adipogenic, chondrogenic and osteogenic differentiation of clonally derived human dermal fibroblasts. Cells Tissues Organs. 2010; 191:105–18. https://doi.org/10.1159/000232157 PMID:19641298

34. Lorenz K, Sicker M, Schmelzer E, Rupf T, Salvetter J, Schulz-Siegmund M, Bader A. Multilineage differentiation potential of human dermal skin-derived fibroblasts. Exp Dermatol. 2008; 17:925–32. https://doi.org/10.1111/j.1600-0625.2008.00724.x PMID:18557932

35. Rosen ED, Walkey CJ, Puigserver P, Spiegelman BM. Transcriptional regulation of adipogenesis. Genes Dev. 2000; 14:1293–307. PMID:10837022

36. Goldring MB, Tsuchimochi K, Ijiri K. The control of chondrogenesis. J Cell Biochem. 2006; 97:33–44. https://doi.org/10.1002/jcb.20652 PMID:16215986

37. Komori T. Regulation of bone development and extracellular matrix protein genes by RUNX2. Cell Tissue Res. 2010; 339:189–95. https://doi.org/10.1007/s00441-009-0832-8 PMID:19649655

38. Krumlauf R. Hox genes in vertebrate development. Cell. 1994; 78:191–201. https://doi.org/10.1016/0092-8674(94)90290-9 PMID:7913880

39. Lehrke M, Lazar MA. The many faces of PPARgamma. Cell. 2005; 123:993–99. https://doi.org/10.1016/j.cell.2005.11.026 PMID:16360030

40. Tang W, Robles AI, Beyer RP, Gray LT, Nguyen GH, Oshima J, Maizels N, Harris CC, Monnat RJ Jr. The

Werner syndrome RECQ helicase targets G4 DNA in human cells to modulate transcription. Hum Mol Genet. 2016; 25:2060–69. https://doi.org/10.1093/hmg/ddw079 PMID:26984941

41. Leone A, Costantini AM, Brigida R, Antoniol OM, Antonelli-Incalzi R, Bonomo L. Soft-tissue mineralization in Werner syndrome. Skeletal Radiol. 2005; 34:47–51. https://doi.org/10.1007/s00256-004-0792-8 PMID:15138723

42. Chen SX, Zhang LJ, Gallo RL. Dermal white adipose tissue: a newly recognized layer of skin innate defense. J Invest Dermatol. 2019; 139:1002–09. https://doi.org/10.1016/j.jid.2018.12.031 PMID:30879642

43. Plikus MV, Guerrero-Juarez CF, Ito M, Li YR, Dedhia PH, Zheng Y, Shao M, Gay DL, Ramos R, Hsi TC, Oh JW, Wang X, Ramirez A, et al. Regeneration of fat cells from myofibroblasts during wound healing. Science. 2017; 355:748–52. https://doi.org/10.1126/science.aai8792 PMID:28059714

44. Zhang Z, Shao M, Hepler C, Zi Z, Zhao S, An YA, Zhu Y, Ghaben AL, Wang MY, Li N, Onodera T, Joffin N, Crewe C, et al. Dermal adipose tissue has high plasticity and undergoes reversible dedifferentiation in mice. J Clin Invest. 2019; 129:5327–42. https://doi.org/10.1172/JCI130239 PMID:31503545

45. Toda T, Satoh M, Sugimoto M, Goto M, Furuichi Y, Kimura N. A comparative analysis of the proteins between the fibroblasts from Werner's syndrome patients and age-matched normal individuals using two-dimensional gel electrophoresis. Mech Ageing Dev. 1998; 100:133–43. https://doi.org/10.1016/s0047-6374(97)00131-0 PMID:9541134

46. Meeker AK, Gage WR, Hicks JL, Simon I, Coffman JR, Platz EA, March GE, De Marzo AM. Telomere length assessment in human archival tissues: combined telomere fluorescence *in situ* hybridization and immunostaining. Am J Pathol. 2002; 160:1259–68. https://doi.org/10.1016/S0002-9440(10)62553-9 PMID:11943711

47. Mourkioti F, Kustan J, Kraft P, Day JW, Zhao MM, Kost-Alimova M, Protopopov A, DePinho RA, Bernstein D, Meeker AK, Blau HM. Role of telomere dysfunction in cardiac failure in duchenne muscular dystrophy. Nat Cell Biol. 2013; 15:895–904. https://doi.org/10.1038/ncb2790 PMID:23831727

48. Ide S, Finer G, Maezawa Y, Onay T, Souma T, Scott R, Ide K, Akimoto Y, Li C, Ye M, Zhao X, Baba Y, Minamizuka T, et al. Transcription factor 21 is required for branching morphogenesis and regulates the gdnf-axis in kidney development. J Am Soc Nephrol. 2018; 29:2795–808. https://doi.org/10.1681/ASN.2017121278 PMID:30377232

49. Ge SX, Son EW, Yao R. iDEP: an integrated web application for differential expression and pathway analysis of RNA-seq data. BMC Bioinformatics. 2018; 19:534. https://doi.org/10.1186/s12859-018-2486-6 PMID:30567491

SUPPLEMENTARY MATERIALS

Supplementary Figures

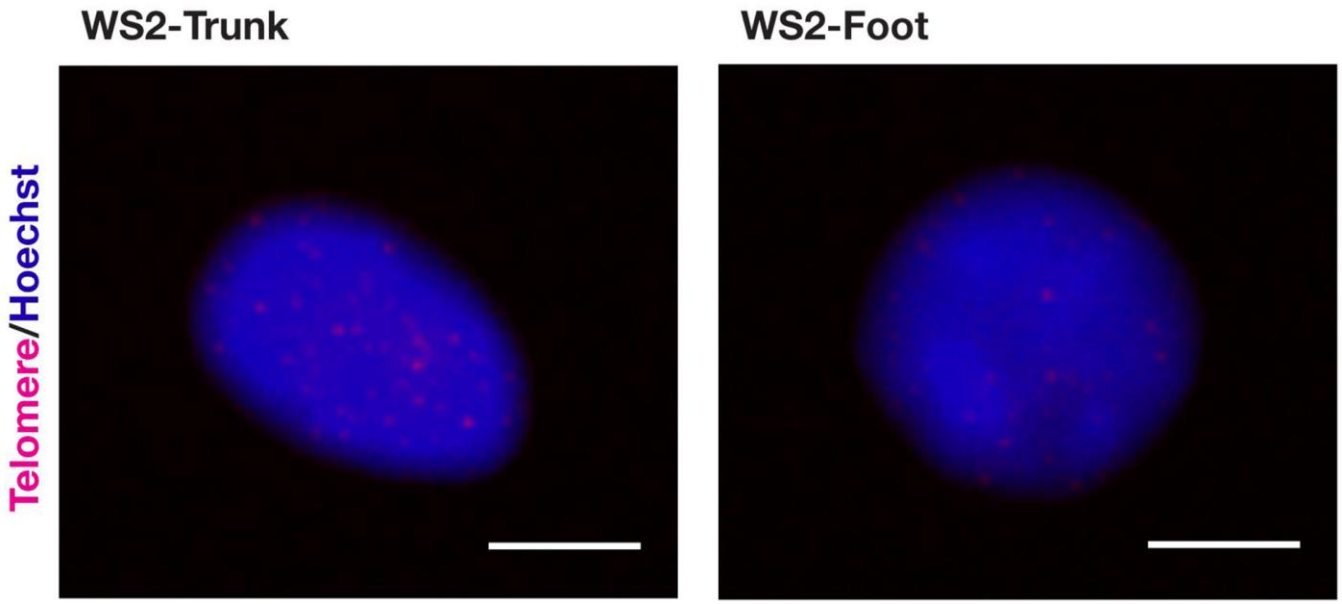

Supplementary Figure 1. Representative image of telomere Q-FISH of WS2. Bar = 10 μm.

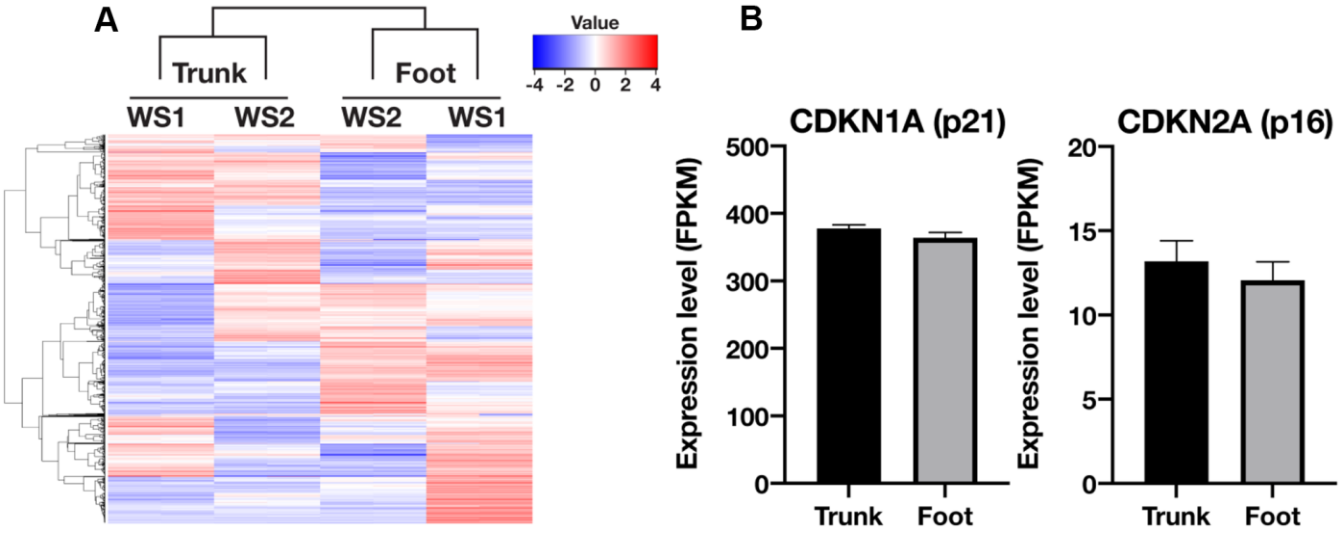

Supplementary Figure 2. Results of transcriptome analysis of the trunk and foot fibroblasts. (**A**) Heatmap of the hierarchical clustering analysis. (**B**) FPKM results of CDKN1A (p21) and CDKN2A (p16). Data are means ± SEM of two patients (technically n=2 in each sample).

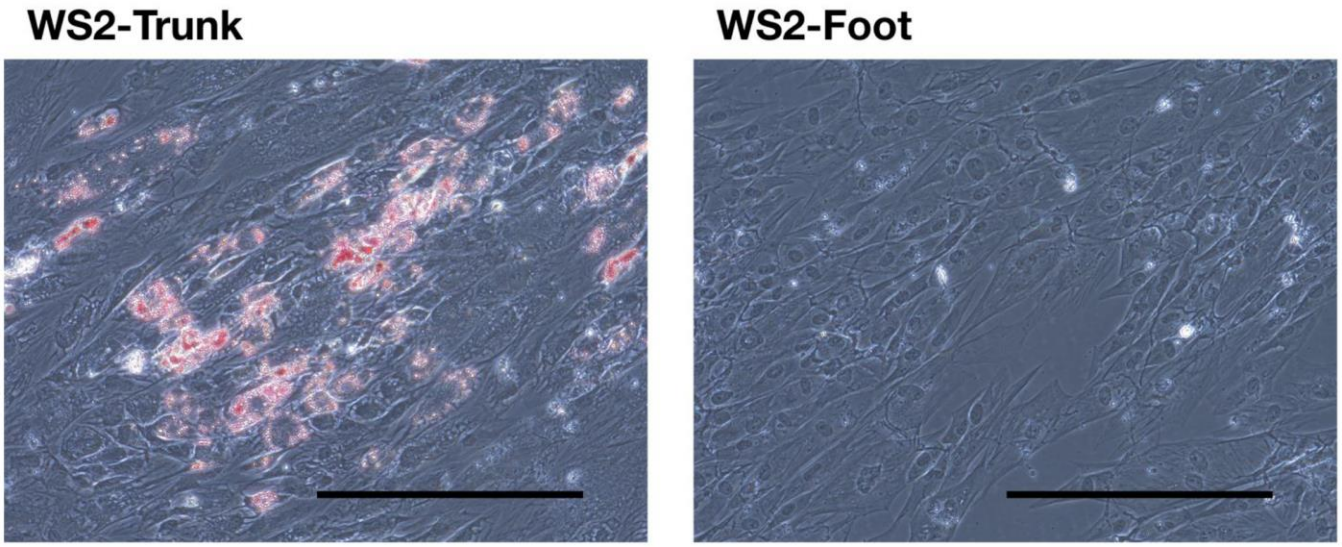

Supplementary Figure 3. Representative images of Oil red O staining two weeks after induction of adipogenesis in the trunk and foot fibroblasts of WS2. Bar = 300 μm.

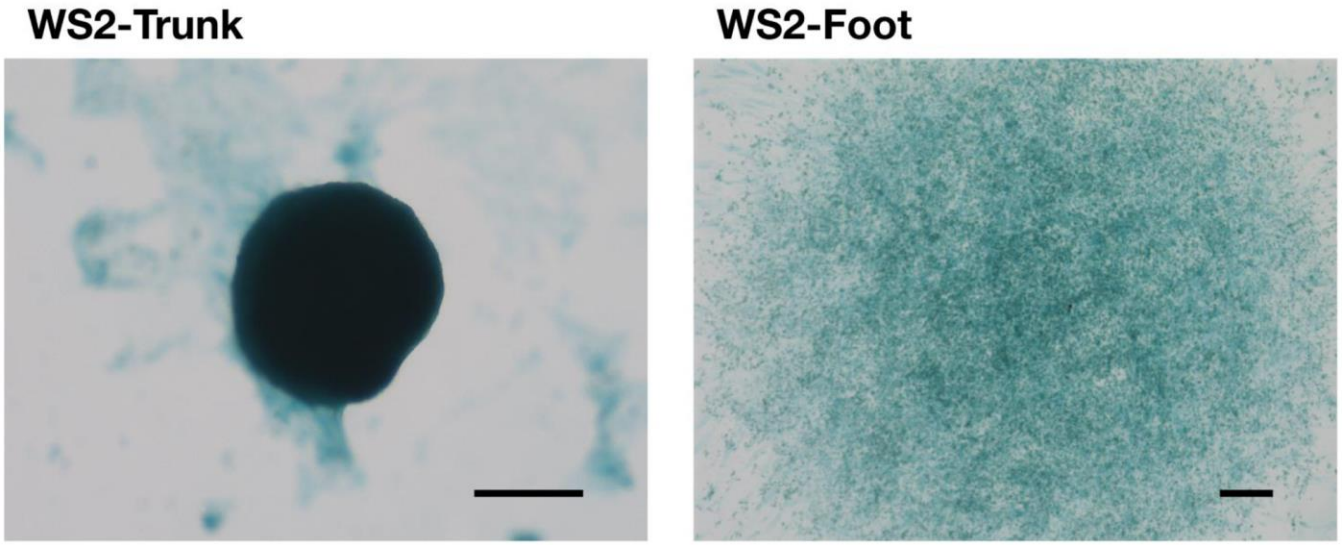

Supplementary Figure 4. Representative images of Alcian blue staining two weeks after induction of chondrogenesis in the trunk and foot fibroblasts of WS2. Bar = 300 μm.

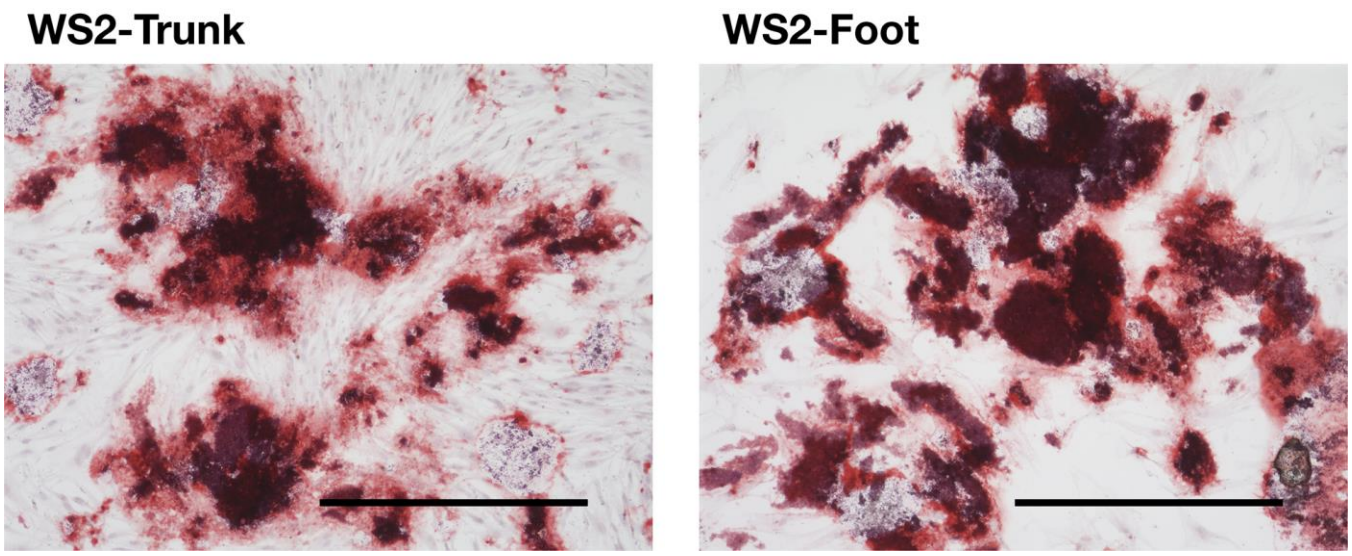

Supplementary Figure 5. Representative images of Alizarin red staining two weeks after induction of osteogenesis in the trunk and foot fibroblasts of WS2. Bar = 300 μm.

Supplementary Tables

Please browse Full Text version to see the data of Supplementary Tables 1–4.

Supplementary Table 1. Raw data of hierarchical clustering analysis heatmap. Each value is represented as log2(FPKM+1).

Supplementary Table 2. Up-regulated genes in Foot fibroblasts. Each value is represented as log2(FPKM+1). Genes are listed in order from high to low of log2(Foot/Trunk). Cutoff: log2(Foot/Trunk) > 1 and FDR < 0.05.

Supplementary Table 3. Down-regulated genes in Foot fibroblasts. Each value is represented as log2(FPKM+1). Genes are listed in order from low to high of log2(Foot/Trunk). Cutoff: log2(Foot/Trunk) < -1 and FDR < 0.05.

Supplementary Table 4. Clinical characteristics of the patients.